Vibration Suppression of Offshore Wind Turbine Foundations using Tuned Liquid Column Dampers and Tuned Mass Dampers

Arash Hemmati[a], Erkan Oterkus[a,1], Mahdi Khorasanchi[b]

[a]Department of Naval Architecture, Ocean and Marine Engineering, University of Strathclyde, 100 Montrose Street, Glasgow G4 0LZ, UK

[b]Department of Mechanical Engineering, Sharif University of Technology, Azadi Ave, Tehran, Iran

ABSTRACT

Highly dynamic nature of the applied loads on flexible and lightly damped offshore wind turbine (OWT) foundations affects the lifetime and serviceability of the system. In this study, the excessive vibration responses of OWTs are minimized using tuned mass dampers (TMD) and tuned liquid column dampers (TLCD). Due to high efficiency of TLCDs and TMDs for certain loading conditions, a combined TLCD-TMD is also utilized to improve the overall performance in a wide range of loading conditions. First, a parametric study was performed that highlights the sensitivity of these structural control devices. The effect of two devices on fixed offshore wind turbine foundations for the benchmark 5MW NREL turbine in various loading patterns was investigated. Then, the model was subjected to stochastically generated wind loading in operational, parked, startup, and shutdown conditions. The results suggest that the standard deviation of the dynamic responses can be greatly reduced with all structural control devices. However, TMDs are more efficient in operational conditions, whereas TLCDs show better performances in parked conditions. This highlights the possibility and efficiency of a combined TLCD-TMD system in which the dynamic responses are minimized efficiently in a wider selection of loading conditions.

[1] Corresponding author:
E-mail address: Erkan.oterkus@strath.ac.uk

Keywords:

Offshore wind turbine, Vibration control, Passive control, Tuned mass damper, Dynamic analysis

1. INTRODUCTION

Wind energy has been one of the most promising renewable energy sources and the offshore wind industry is growing fast due to its more reliable wind resources compared to onshore wind. However, the challenges in the development of offshore wind need to be addressed. Foundations of offshore wind turbines contribute more to the total cost of the system at an amount of 15-25% (Seidel, 2014). Therefore, OWT foundations need to be optimized in order to compete with other renewables. Since OWTs are subjected to various environmental dynamic loading conditions such as wind, wave, and current in conjunction with excitation loading of the turbine itself, their highly dynamic oscillations can be suppressed by introducing higher damping. Vibration control systems developed in other fields such as civil and mechanical engineering can be used in offshore wind systems to mitigate the oscillation and consequently improve the lifetime and serviceability of the system. Three main structural control systems such as active, passive, and semi-active have been used in a number of structures (Symans and Constantinou, 1999). Passive control systems can enhance structural damping, stiffness, and strength without employing force devices, complex sensors, and instrumental equipment. The main outcome of using a passive control system is to minimize the oscillation of the system. There are various damping devices such as tuned mass dampers, tuned liquid dampers, and fluid dampers. Tuned mass dampers have been implemented in tall buildings, towers and bridges and its effectiveness during earthquakes has been well proved (Kareem et al., 1999). Due to simplicity and effectiveness of TMDs, they have been popular in the wind industry and there have been a number of studies focusing on wind turbine tower using TMD (Lackner and Rotea, 2011a, 2011b; Stewart and Lackner, 2013; Stewart and Lackner, 2014; Yilmaz, 2012). Among these, Stewart and Lackner (2014) examined the impact of passive tuned mass dampers considering wind-wave misalignment on offshore wind turbine loads for monopile foundations. The results demonstrated that TMDs are efficient in damage reduction of towers, especially in side-side directions. G. Stewart and Lackner (2013) in another study investigated the effectiveness of TMD systems for four different types of platforms including monopile, barge, spar buoy, and tension-leg and they observed tower fatigue damage reductions of up to 20% for various TMD configurations. There have also been some investigations on the impact of TMDs on wind turbine blades (Ming He et al., 2014; Fitzgerald and Basu, 2013; Fitzgerald et al., 2013). The use of active tuned mass dampers for control of in-place vibrations of wind turbine blades was studied by (Fitzgerald et al., 2013) and they demonstrated promising results

especially for high turbulent loadings. In addition, Brodersen et al. (2017) investigated the effect of an active tuned mass damper (ATMD) on the tower vibrations in frequency and time domains. The actuator force used in their study is controlled by the absolute displacement of the tower and the relative velocity of the damper mass. They concluded that the ATMD provides a considerable decrease in the frequency response. Their results showed that the ATMD is also superior in reducing the vibrations in transient conditions. Furthermore, Fitzgerald et al. [2] incorporated an ATMD into the tower of an onshore wind turbine and estimated the improved reliability of the system under stochastically generated wind loads. Their results showed a significant improvement in reliability of the system at the rated wind speed. The viability of application of semi-active tuned mass dampers to control undesired flapwise vibrations in wind turbine blades was investigated by (John et al., 2011). They proposed a frequency-tracking algorithm based on the short-time Fourier transform technique in order to retune the frequency of the tuned mass damper. Furthermore, using multiple tuned mass dampers (MTMD) was proposed to improve the performance of vibration control system (Dinh and Basu, 2015). They investigated the application of MTMDs for structural control of nacelle and tower of spar floating wind turbines and concluded that MTMDs are more efficient in displacement reductions. Then using MTMDs to control excessive vibration excited by higher modes of offshore wind turbine tower under multi-hazard was proposed by (Zuo et al., 2017) and they concluded that installing the control devices along the tower improve the performance of the system. More recently, Sun (2018) investigated using semi-active MTMDs for mitigating dynamic response of an offshore wind turbine considering the stiffness reduction occurring after earthquake motions.

Tuned Liquid Column Dampers (TLCDs) are another popular vibration control system that has been used in civil engineering due to its easier maintenance requirements and costs. Bauer (1984) was one of the first to propose using a container filled with liquids to mitigate the oscillation of a cantilever beam. The application of this kind of structural control device in buildings has been studied by (Sakai et al., 1989; Welt and Modi, 1992). Fujino et al. (1992) and Lepelletier and Raichlen (1988) further investigated the behavior of the fluid motion in an oscillating rectangular tank. With regard to optimization of TLCDs, Yalla and Kareem (2000) proposed a new approach to find the optimal parameters of tuned liquid column dampers in order to improve their performance. The effectiveness of TLCDs in structural control of wind turbine systems has been studied by a number of researchers (Colwell and Basu, 2009; Ghaemmaghami et al., 2015; Arrigan and Basu, 2007; Mensah and Dueñas-Osorio, 2014; Zhang et al., 2015). Ghaemmaghami et al. (2015) concluded that tuned liquid dampers are effective for small amplitude excitations. Colwell and Basu (2009) studied effects of TLCD on offshore wind turbine systems to suppress the excessive vibration and found that TLCD can minimize vibration up to 55% of peak response compared to the uncontrolled system. Mensah and Dueñas-Osorio (2014) investigated reliability improvement of wind turbine system using TLCD and their results show a considerable reduction in displacement and bending moment in the tower.

There have also been studies on the effectiveness of TLCD on vibration suppression of wind turbine blades that achieved improved results (Arrigan and Basu, 2007; Zhang et al., 2015).

Previous studies have almost exclusively focused on the application of tuned mass dampers or tuned liquid column dampers separately and no previous research has investigated using both devices simultaneously for offshore wind turbines. Due to turbulent nature of environmental loading, offshore wind turbines oscillate with low and high amplitude excitations and therefore a structural control system efficient in suppressing a wide range of amplitude excitations is more suitable. Since TLCDs perform better under low amplitude vibrations (Colwell and Basu, 2009; Ghaemmaghami et al., 2015) and TMDs dissipate high amplitude vibrations more effectively, a combination system of TLCDs and TMDs is utilized in this research in order to suppress a wider range of amplitude vibrations more efficiently. Moreover, previous studies are limited to study of structural control devices for offshore wind turbines in operational and parked conditions and other special loading conditions such as startup and shutdown conditions are rarely studied in the literature. To fill this gap, in this research not only operational and parked but also startup and shutdown conditions are assessed. This study focuses on the jacket foundations using multiple lumped mass model and the baseline 5MW NREL turbine is considered (Jonkman, 2009). First, free decay vibration, monotonic, impulse and harmonic loadings are assessed. Then, a number of stochastically generated wind loadings in operational, parked, startup, and shutdown conditions at various wind speeds are considered to demonstrate the impact of the mentioned structural control devices. Finally, a parametric study is carried out to investigate the effects of various parameters on the performance of the structural control devices.

2. NUMERICAL MODEL

2.1. Tuned Liquid Column Dampers

TLCDs are composed of a U-shaped tube that is partially filled with liquid and dissipate vibration energy using the oscillation of the liquid between two columns. This oscillation of the liquid enables the system to re-establish equilibrium and dampen out the vibration. Fig. 1 shows a schematic configuration of a TLCD attached to the main structure.

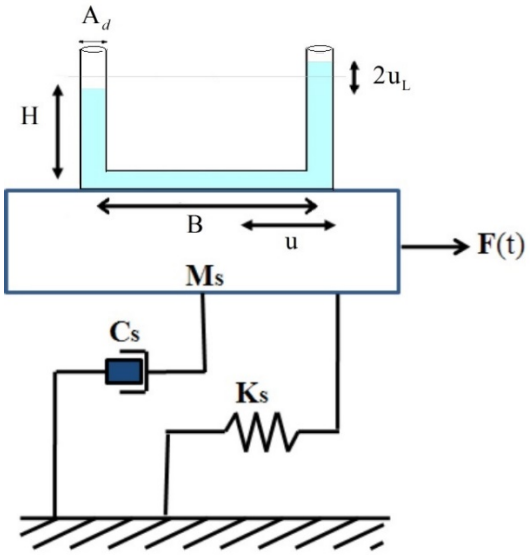

Fig. 1. Schematic diagram of TLCD model

Two major assumptions are used in order to derive dynamic equations of TLCDs: (1) the liquid is incompressible and no pressure is created due to the oscillation of the liquid in the tube, (2) the sloshing of the liquid surface may be ignored as it is negligible compared to the sloshing of the whole body of water. The equation of motion of a U-shaped pipe attached to a structure for controlling vibration of the structure was developed by (Sakai et al., 1989) and can be described as:

$$\rho A_d L_T \ddot{u}_L + \frac{1}{2}\rho A \xi |\dot{u}_L| \dot{u}_L + 2\rho A g u_L = -\rho A B \ddot{u} \tag{1}$$

where ρ is the density of the fluid, A_d is the cross-sectional area of the tube, B is the horizontal distance between two columns, g is the acceleration due to gravity, u_L is the change in the elevation of the liquid inside the columns and u is the horizontal deflection at the base of TLCD where it is attached to the OWT systems that can be located in nacelle, tower or transition piece. The overdot denotes differentiation with respect to time. ξ is the non-linear coefficient of head loss which is dependent on the opening ratio of the orifice ψ (ratio of the diameter of the orifice to the diameter of the horizontal tube). ξ can be calculated from the empirical formula developed from experimental results (Wu et al., 2005):

$$\xi = (-0.6\psi + 2.1\psi^{0.1})^{1.6}(1-\psi)^{-2} \tag{2}$$

Eq. (1) can be rewritten by dividing by the mass of the liquid as

$$u_L + \frac{\xi}{2L}|u_L|u_L + \omega_L^2 u = -\alpha u \tag{3}$$

in which $L_T = B + 2H$ is the total length of the tube, $\alpha = B / L_T$ is the ratio of horizontal length to the total length, $\omega_L = \sqrt{2g / L_T}$ is the natural circular frequency of the TLCD.

The equation of motion of the main structure with n-degrees of freedom attached to the TLCD can be expressed as:

$$M_s X + C_s X + K_s X = P(t) - \rho A B u_L R - \rho A L_T u R \tag{4}$$

in which $X = \{x_1, x_2, ..., x_n\}$ is the horizontal displacement vector of the main structure, $R = \{1, 0, ..., 0\}^{\mathrm{T}}$ is a constant vector. K_s, M_s, and C_s are the n-dimensional stiffness, mass, and damping matrices of the main structure, respectively. $P(t)$ is n-dimensional vector of external force applied to the main structure.

The tuned liquid column damper is tuned to the first natural frequency of the system by tuning ratio $\gamma = \omega_L / \omega_s$ which is controlled by the mass ratio $\mu = m_{TLCD} / m_s$. ω_L and ω_s are the frequency of the TLCD and natural frequency of the main structure, respectively. m_{TLCD} and m_s are the mass of TLCD and the mass of the main structure, respectively.

The equation of motion of the TLCD in conjunction with the main structure's equations is solved simultaneously in the nonlinear time domain using Newmark method (Newmark, 1959) in order to consider the dynamic motion of the TLCD.

2.2. Tuned Mass Damper Systems

A tuned mass damper (TMD) is a device that consists of a mass, a damper, and a mass attached to a structure to control the dynamic vibration. The key aspect of a TMD is that its frequency needs to be tuned to a particular structural frequency so that it dampens out the vibration when that frequency is excited. The theory of multiple degrees of freedom (MDOF) systems using tuned mass dampers are illustrated and presented in the following section.

The governing equations for the MDOF system in Fig. 2. are given as:

$$
\begin{aligned}
&m_1u_1 + c_1u_1 + k_1u - k_2(u_2 - u_1) - c_2(u_2 - u_1) = p_1 - m_1u_g \\
&m_2u_2 + c_2(u_2 - u_1) + k_2(u_2 - u_1) - k_3(u_3 - u_2) - c_3(u_3 - u_2) = p_2 - m_2u_g \\
&\qquad\qquad\vdots \\
&m_du_d + c_du_d + k_du_d = -m_d(u_n + u_g)
\end{aligned}
\tag{5}
$$

where m_i, c_i, k_i, u_i, and p_i are mass, damping, stiffness, deflection, and point load for different degrees of freedom of main structure ($i = 1, 2, ..., n$), and m_d, c_d, k_d, and u_d are mass, damping, stiffness, and deflection for the TMD attached to the main structure.

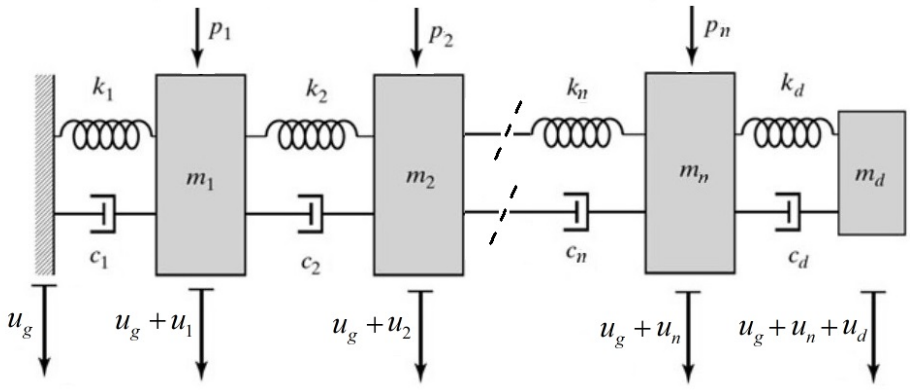

Fig. 2. Multi degrees of freedom system equipped with a TMD

The integrated dynamic equations of offshore wind turbine can be expressed as:

$$
\begin{bmatrix} M_s & \\ & m_d \end{bmatrix}\begin{bmatrix} X_s \\ u_d \end{bmatrix} + \begin{bmatrix} C_s & \\ & c_d \end{bmatrix}\begin{bmatrix} X_s \\ u_d \end{bmatrix} + \begin{bmatrix} K_s & \\ & k_d \end{bmatrix}\begin{bmatrix} X_s \\ u_d \end{bmatrix} = \begin{bmatrix} P(t) \\ -m_du_n \end{bmatrix} - \rho ABu_L\begin{bmatrix} R \\ 0 \end{bmatrix} - \rho AL_Tu\begin{bmatrix} R \\ 0 \end{bmatrix} \tag{6}
$$

The schematic layout of integrated TLCD-TMD located in the nacelle is shown in Fig. 3.

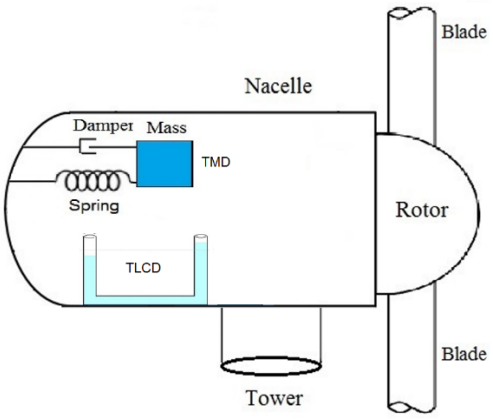

Fig. 3. Schematic layout of TLCD-TMD in the nacelle

2.3. Main Structural Model

The stiffness and mass matrices were built using a system based on the multi-degree-of-freedom lumped-mass model in which the complete offshore wind turbine system includes the piling system, jacket substructure, transition piece, tower, hub, and blades as depicted in Fig. 4a. For each level, the area moment of inertia I_i contributed by all the vertical members of the structure can be expressed as:

$$I_i = \sum I_{ij} \tag{7}$$

where I_{ij} is the area moment of inertia for each structural member at the same level. For each member such as jacket leg/brace and tower, the area moment of inertia can be obtained as

$$I_{ij} = \frac{\pi}{4}(R^4 - (R-T)^4) \times \cos(\theta) \tag{8}$$

in which R and T are the radius and thickness of the member; θ is the angle between the member and the horizontal direction. The stiffness matrix and mass matrix are based on the discrete system for a multi-degree-of-freedom system made of *n* masses as shown in the Appendix (Eddanguir and Benamar, 2013). Table 1 tabulates the material properties of the steel used in the tower and jacket of the offshore wind turbine. The density of the steel in the tower is taken higher than that of the steel to take into account the weight of the paint, bolts, welds, and flanges which are not modeled directly (Jonkman, 2009).

Table 1 Material Properties

Component	Density (kg/m^3)	Young's modulus (GPa)	Poisson's ratio
Tower	8500	210	0.3
Jacket	7850	210	0.3

2.4. Turbine Model Description

In this study, NREL 5 MW wind turbine was considered as it is widely used as the turbine for benchmark studies (J. M. Jonkman and Buhl Jr, 2005). This turbine is supported by baseline jacket foundation designed during the UpWind project (Vorpahl, 2013). The general configuration of the turbine is shown in Fig. 4b and its particulars can be found in Table 2.

Table 2 Properties of NREL 5MW baseline turbine

Rating	5MW
Rotor Orientation	UpWind, 3 Blades
Control System	Variable Speed, Collective Pitch
Rotor, Hub Diameter	126.0 m, 3.0 m
Hub Height	90.0 m
Cut-In, Rated, Cut-Out Wind Speed	3 m/s, 11.4 m/s, 25 m/s
Cut-In, Rated Rotor Speed	6.9 rpm, 12.1 rpm
Rotor Mass, Nacelle Mass	110,000 kg, 240,000 kg
Nacelle Dimensions	18 m*6 m *6 m

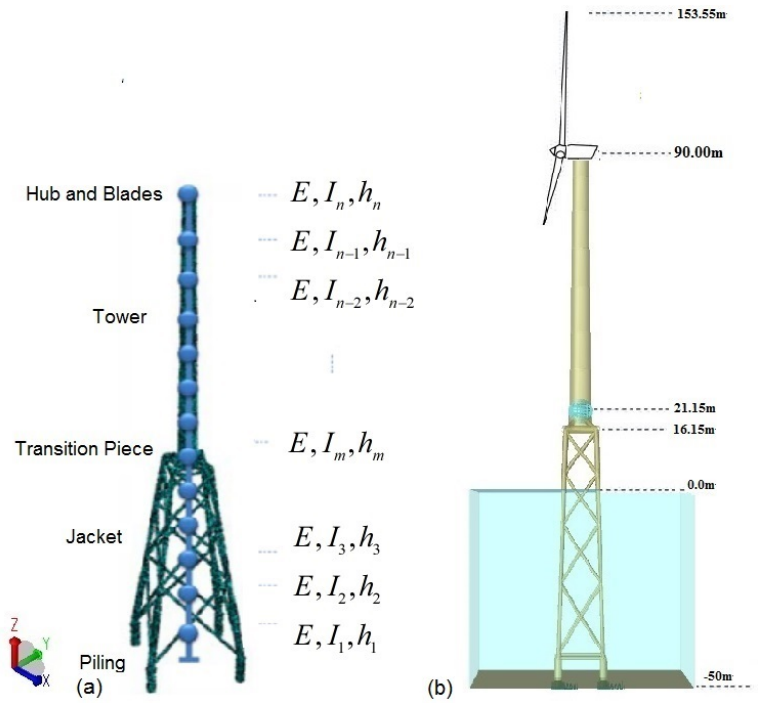

Fig. 4 (a) 3-D schematic (b) configuration dimensions of the offshore wind turbine system

3. NUMERICAL RESULTS AND DISCUSSION

3.1. Basic Loading Functions

First, the complete offshore wind system equipped with TMD, TLCD and combined TLCD-TMD tuned to the first natural frequency of the system is subjected to an initial perturbation where the tower is displaced and allowed to oscillate freely. Three values of mass of the controller as 10 tons, 20 tons, and 40 tons are selected and the optimal parameters are obtained by tuning the structural control devices to the first natural frequency of the system. The TMD mass ratios corresponding to aforementioned masses are 1.1%, 2.2% and 4.4% respectively. The optimal tuning ratio is set as $\gamma = 1/(1+\mu)$. The parameters are tabulated in Table 3. For TLCDs, it is assumed that the type of the liquid is water. However, using liquids with higher density such as glucose solution with a density of 1540 kg/m^3 results in 35% saving in the space required. The TMD and the TLCD are assumed to be installed in the nacelle and in the tower at the highest level, respectively.

.

Table 3 Optimal vibration controller parameters for the NREL 5 MW supported by a jacket

		TMD			TLCD				
Mass (kg)	Mass ratio	$k_d\,(N/m)$	$c_d\,(N/(m/s))$	$\omega_d\,(Hz)$	α	γ	μ	ξ	ψ
10,000	1.1%	41258	647	0.323	0.7	0.986	0.014	4.69	0.3
20,000	2.2%	80190	1275	0.319	0.7	0.972	0.029	4.69	0.3
40,000	4.4%	151915	2481	0.310	0.7	0.946	0.057	4.69	0.3

The time history of the deflection at the top of the tower shows how quickly the vibration is dampened out in Fig. 5. As can be seen in this figure, increasing the mass of TMD and TLCD improves the damping capacity of the controller. Fig. 5c compares the performance of a TMD, a TCD and a combined TLCD-TMD with a mass of 20 tons under free decay vibration. As the figure indicates combining two devices together (TLCD-TMD) can control the free decay vibration more effectively.

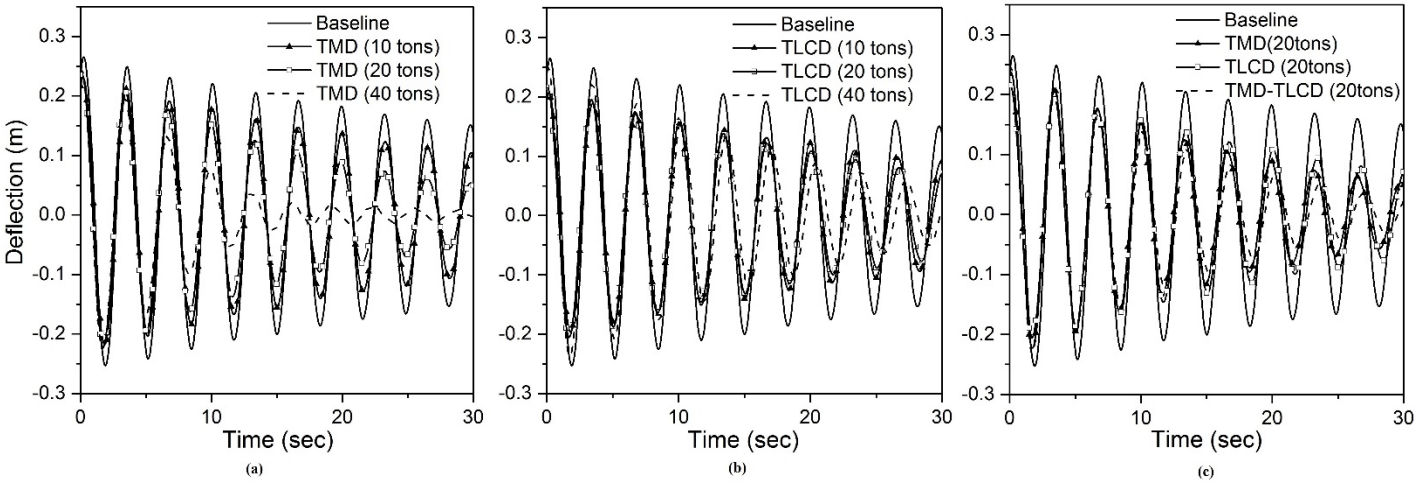

Fig. 5. Free decay vibrations (a) TMD systems (b) TLCD systems (c) combined systems

Then, using logarithmic damping formula, the output damping ratio produced by damping devices is calculated by extracting the output damping of the uncontrolled system (baseline) from that of the controlled system according to the following formula;

$$\xi_{Damper} = \xi_{Controlled} - \xi_{Baseline} \tag{9}$$

Table 4 Output damping ratios produced from controller devices (%)

Mass (tons)	Mass ratio	TMD	TLCD	TLCD-TMD
10	1.1%	1.33	1.46	1.92
20	2.2%	2.54	2.21	4.43
40	4.4%	4.35	3.64	6.34

Table 4 tabulates the extra damping ratio produced when the controller devices are used. The output damping ratio for the combined device is much higher than the separate devices. For instance, the output damping ratio of TLCD-TMD with 20 tons is 43% higher than a TMD with a mass of 20 tons. Since free decay vibration oscillates under the natural frequency of the system which is not the case for operational cases, a study on the vibration control in the realistic operational case is more representative of the effectiveness of these systems and it is discussed in section 3.4 of this paper. The time history of the deflections for three different loads (monotonic, impulsive and harmonic) and the effect of the controller devices on the deflection of the top of the tower is examined. The time to reach ultimate load in monotonic loading, the duration of the impulsive loading, and the period of the harmonic loading are shown as T_d (Fig. 6) and were chosen as 1, 3.05 and 5 sec. The reason for choosing these values is to have the period of loading less, equal and larger than natural period of the whole system. In order to show the efficiency of control devices, structural response of uncontrolled OWT is compared with the systems equipped with damping devices. In these cases, the mass of TMD, TLCD and combined TLCD-TMD was kept 20 tons and other parameters were chosen in a way to tune to the natural frequency of the system according to Table 3.

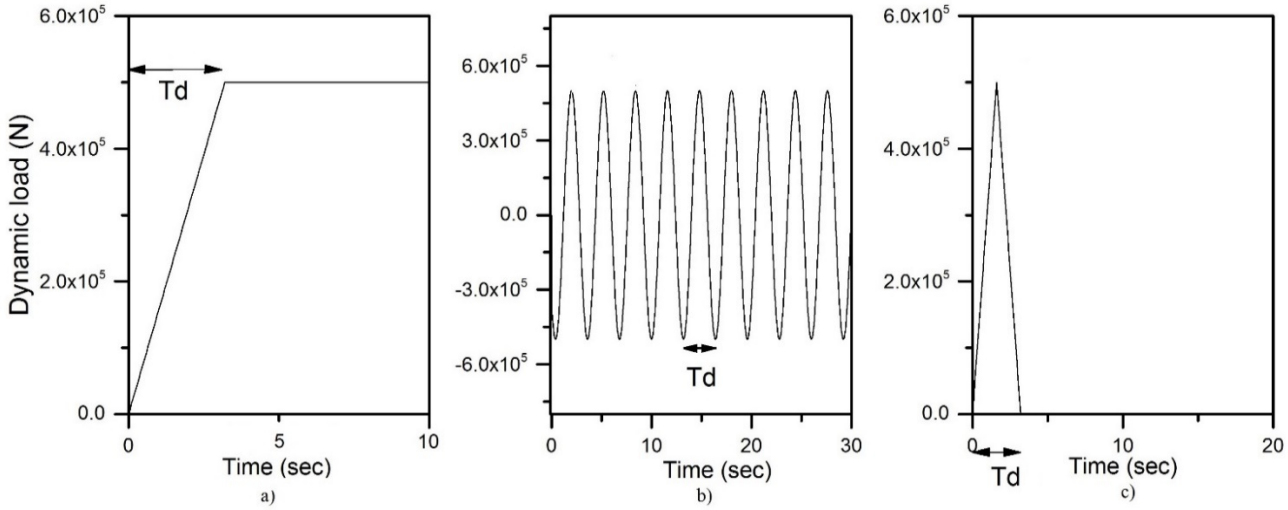

Fig. 6. Loading functions in numerical examples (a) monotonic (b) harmonic (c) impulsive

The deflections for these loadings are shown in Fig. 7-9. For monotonic loading, the results show that controller devices reduce amplitudes of deflection in the transition period and this reduction is more pronounced when the time to reach the ultimate load is smaller as this makes the loading more dynamic. This trend again can be seen for impulsive loading similar to monotonic loading.

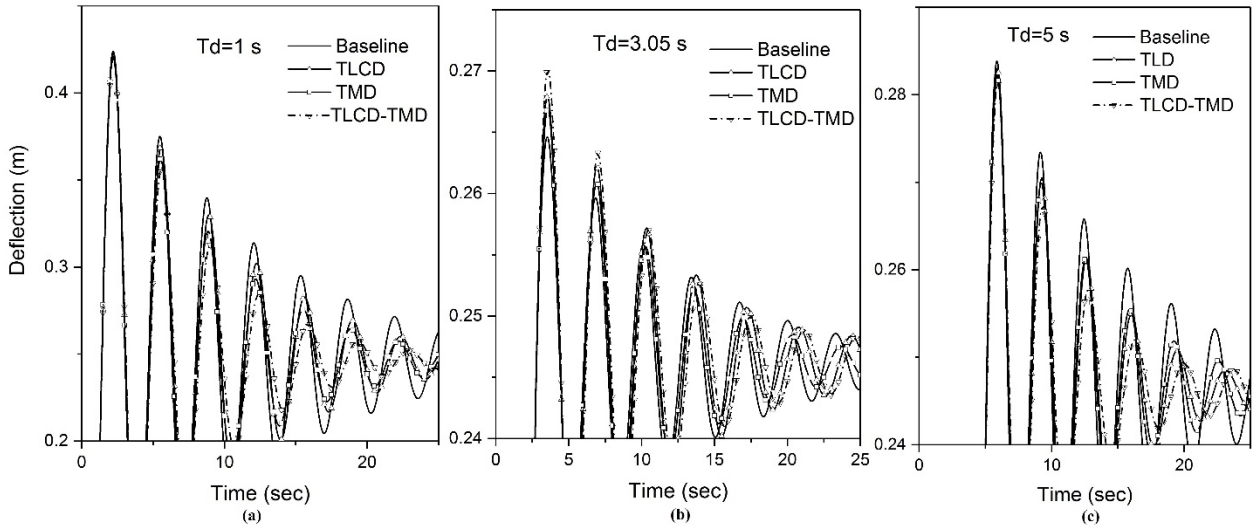

Fig. 7. Structural responses under monotonic loading (a) T_d =1 sec **(**b) T_d =3.05 sec **(**c) T_d =5 sec

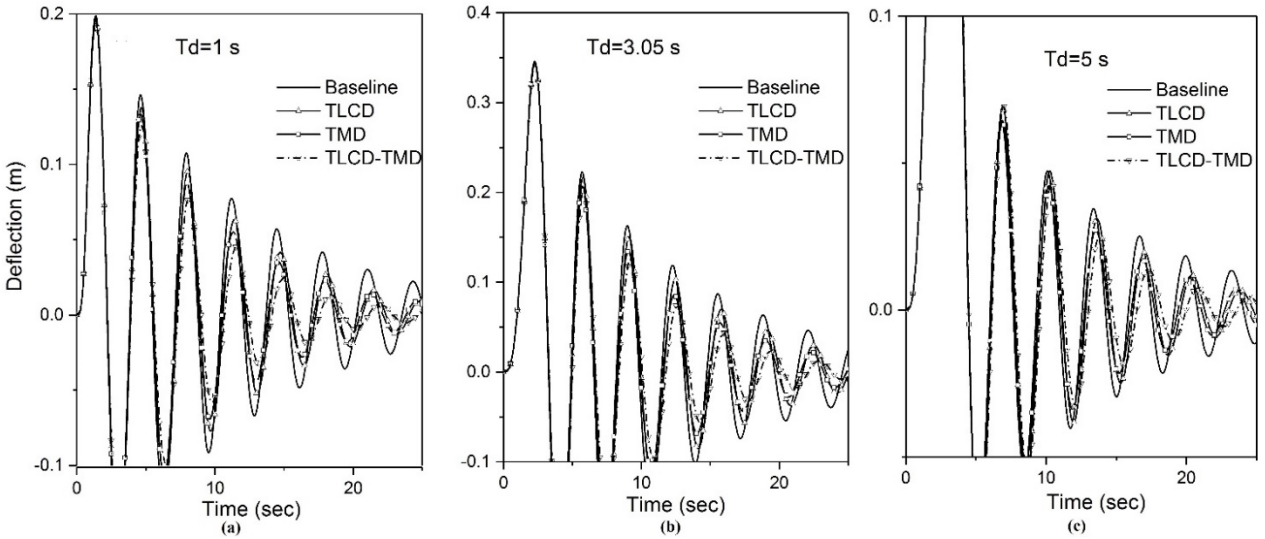

Fig. 8. Structural responses under impulsive loading (a) T_d =1 sec **(**b) T_d =3.05 sec **(**c) T_d =5 sec

For harmonic loading, control devices reduce the amplitude of vibration considerably when the structure is excited with loading frequency equal to the natural frequency of the structure (Fig. 9b) and this is more pronounced for combined TLCD-TMD, with 17% reduction in the amplitude of the vibration. However, when the period of harmonic loading is lower than natural period of OWT (Fig. 9a), the control devices only have an impact in the transient period and it has negligible effects in the steady state of the time history. For harmonic loading with a larger period (Fig. 9c), the amplitude of vibration even slightly increases due to increase in the mass of the whole system and subsequently decrease in natural frequency.

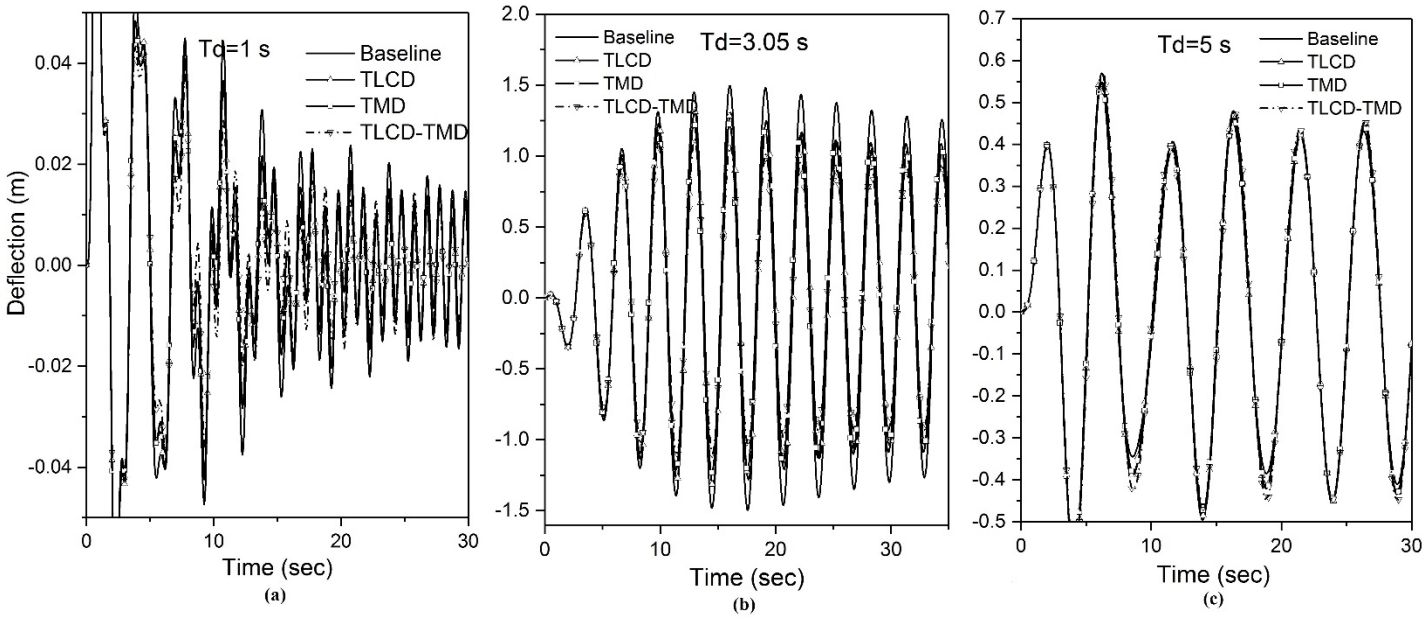

Fig. 9. Structural responses under harmonic loading (a) T_d =1 sec (b) T_d =3.05 sec (c) T_d =5 sec

3.2. Parametric Study of TMD

In this section, harmonic forced vibration simulations were performed by a series of frequency loading with different TMD masses. The model was excited with $F = F_{st} \sin \omega t$, in which F_{st} is the static amplitude of the harmonic excitation and ω is the angular frequency of the excitation. The static amplitude F_{st} was kept constant and the excitation frequency swept in the range of 0.1 Hz to 1 Hz.

In order to scrutinize the responses relative to the baseline model without TMD, the results of models with TMD are normalized by the results without TMD and relative change in responses is demonstrated in Fig. 10. It shows that there is a maximum of 35% decrease in the amplitudes for the TMD with a mass of 10 tons when the structure is excited with loading frequency equal to the natural frequency of the whole system. This relative change increases with higher TMD masses, with 80% decrease for a TMD with 40 tons mass. Also, the sharp peak of the curves slightly shifts to lower frequencies with increase in mass of TMD as it leads to decrease in natural frequency of the system. Beyond the suppression band, the TMD with 10 tons has a slight negative effect. However, heavier TMDs can increase the vibration responses up to 60% if loading frequency is out of the suppression band. Therefore, this highlights the importance of correct tuning of TMDs especially for heavier TMDs.

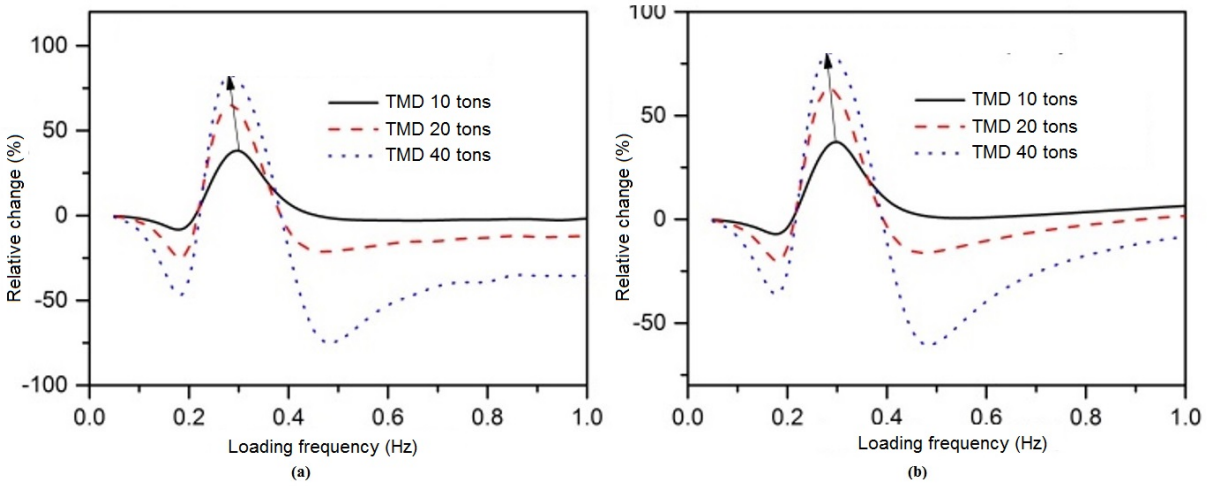

Fig. 10. Relative change of (a) amplitude (b) standard deviation of deflection for different TMD masses

In order to investigate the effects of parameters of TMDs, simulations were run with different TMD spring stiffness and damping and the standard deviation of the results for each time history was obtained and then a surface responses plot was built as depicted in Fig. 11a. This graphical representation of TMD parameters is useful in finding the optimal values and to find out how TMD's efficiency changes. It should be noted that TMD mass was kept constant (20 tons) and only TMD stiffness and damping changes. As the stiffness of TMD changes, the frequency of TMD changes, therefore it is expected that stiffness is a more important parameter in the surface responses plot and the responses are minimum when the stiffness is around 70000 N/m. Regarding damping values, it can be seen that an increase in damping reduces responses. However, this change is more pronounced in lower TMD stiffness. Fig. 11.a displays a linear surface response plot in which a clear optimal value can be found. This surface plot was built for the model without position constraints.

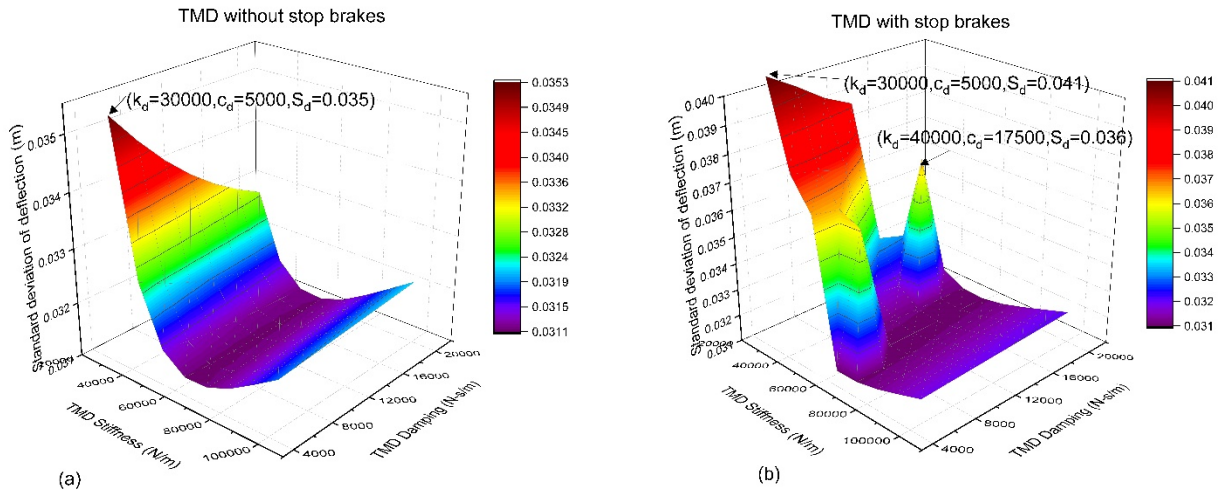

Fig. 11. 3D surface of standard deviation for the system (a) without stop brakes (b) with stop brakes

Since there is a limitation in space in the nacelle and the tower, position constraints should be modeled as stop brakes on the stroke of TMDs. The inclusion of stroke limiter is vital especially for floating offshore wind turbines in which there are larger deflections at the nacelle level. Hu and He (2017) investigated an active mass damper system with a stroke limiter in which the strokes are limited. In this research, stop brakes are incorporated in the model as a spring which comes into contact with the TMD at a certain distance. The stiffness value of this stop brake and the maximum of stroke are two parameters in modeling space constraints. The maximum of stroke is assumed as 2.0 m and the stiffness value is assumed as 200 KN/m. After including this stop brake into the model, simulations were performed and surface response plot was constructed as in Fig. 11b. It can be seen that the surface plot is nonlinear and this nonlinearity is due to the effect of stop brakes. Furthermore, it is clear that the standard deviation of deflection increases for the case with stop brakes compared with the case without stop brakes. For instance, for a TMD stiffness of 30000 N/m and a TMD damping of 5000 N-s/m, the standard deviation increases from 0.035m to 0.041m, resulting in 17% increase in the standard deviation of dynamic responses.

3.3. Parametric Study of TLCD

This section describes a parametric study of controlled systems using TLCDs. First, the effect of the mass ratio of TLCD μ on the standard deviations of deflections is displayed in Fig. 12a, in which it can be observed that higher TLCD mass ratios reduce the

standard deviation of time histories more significantly under loading frequency equal to the natural frequency of the system. In addition, the suppression bandwidth of loading frequency is wider for higher mass ratios. For instance, the suppression bandwidth for the TLCD with the mass ratio of 0.5% is 0.27-0.33Hz, and it increases to a wider bandwidth of 0.24-0.35Hz when the mass ratio is increased to 2%; with approximately twice wider range of frequencies being suppressed. The normalized standard deviation for TLCDs with different ratios of the liquid horizontal length to its total length (B/L) is depicted in Fig. 12b and suggests longer horizontal length of TLCDs weakens the dynamic responses more effectively and also it leads to wider suppression bands in which wider range of loading frequencies can be suppressed.

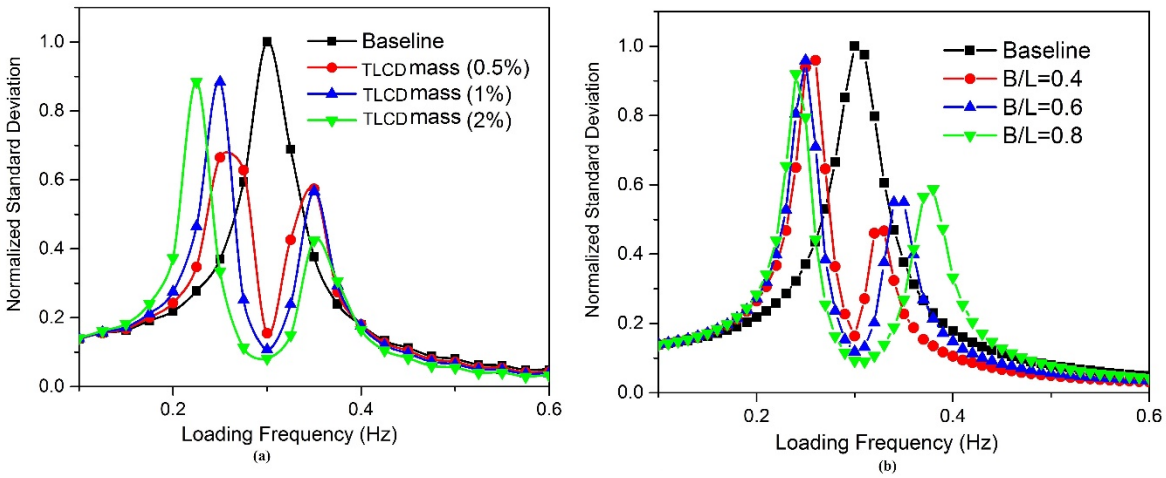

Fig. 12 Normalized standard deviation (a) different mass ratios (b) different B/L ratios

3.4. Stochastic Loading

As harmonic loading is not the realistic loading pattern due to highly random nature of wind loading caused by turbulence, it is vital to investigate the behavior of the structural control devices in stochastic wind loading. This section focuses on stochastic time history using stochastic loading calculated per IEC standard (Commission, 2009) for operational and non-operational load cases. The wind speed acting on the system can be represented by a constant mean wind load $\overline{v}$, and a turbulent wind component $\hat{v}(t)$, $v(t) = \overline{v} + \hat{v}(t)$. The mean velocity $\overline{v}(z)$ is calculated using the logarithmic wind profile as:

$$\bar{v}(z) = V_{ref} \frac{\log(z / z_0)}{\log(H_{ref} / z_0)} \tag{10}$$

where V_{ref} is the mean velocity at the reference height $H_{ref} = 90m$, z is the vertical coordinate, and z_0 is the roughness length.

The Kaimal spectrum (Kaimal et al., 1972) is adopted in this study to calculate the turbulent wind velocity and can be expressed as

$$S_v(f) = \frac{4I^2 L_k}{(1 + 6fL_k / \bar{v})^{5/3}} \tag{11}$$

where *I* is the wind turbulence intensity, f is the frequency (Hz), and L_k is the integral scale parameter.

The wind loadings at different locations are different but with certain similarities, which can be defined with the spatial correlation effect. To model the spatial dependency of the wind velocity at different locations, the cross power spectral density (PSD) function of wind velocity between locations *k* and *l* is defined as:

$$S_{v_k v_l}(f) = Coh(k,l;f)\sqrt{S_{v_k v_k}(f) S_{v_l v_l}(f)} \tag{12}$$

in which $S_{v_k v_k}$ and $S_{v_l v_l}$ are the wind velocity auto spectra at points *k* and *l*, respectively, as defined by Eq. (11), and $Coh(k,l;f)$ is the spatial coherence function from IEC (Commission, 2009) which is expressed as:

$$Coh(k,l;f) = \exp(-a\sqrt{(\frac{fl}{\bar{v}_{hub}})^2 + (\frac{0.12L}{L_c})^2}) \tag{13}$$

in which *a* is the coherence decrement, *L* is the distance between point*s k* and *l* on the grid, L_c is coherence scale parameter, and $\bar{v}_{hub}$ is the mean wind speed at the hub.

In the present study, the air density, the coherent decrement, the coherence scale parameters, the roughness length, and the drag coefficient are taken as 1200 kg/m^3, 12, 340.2m, 0.005, and 1.2 respectively. Then a 3D wind velocity field with 961 points (31 × 31) which covers the rotors is generated based on Eqs. (10)-(13) using Turbsim code (B. J. Jonkman, 2009). Next, the time history loading generated in FAST was imported to the code developed in MATLAB. In order to consider the randomness of loading six 10 minute stochastic time histories with six different seed numbers were analyzed according to the standards (Commission, 2009) and the average of the responses is obtained for different wind speeds. The responses include an average of peaks and standard deviation for six random seeds at each wind speed bin.

3.4.1. Operational Loading

First, the effect of structural control devices on the vibration of the system under operational loading was studied. Fig. 13a shows peak values of deflection and it can be seen that the maximum of the peak values occurs at rated wind speed due to the fact that maximum thrust force occurs at the rated wind speed in collective pitch control type of turbines. In partial loading conditions (wind speed lower than the rated wind speed), the optimal TMDs have a slight suppressive effect. However, TMD's performance in reducing peaks of deflection is better in fully loaded conditions (wind speed higher than rated wind speed). Fig. 13b shows the standard deviation of responses and the figure suggests that the standard deviation increases in higher wind speeds. Also, the difference between the curves with and without TMDs increases as wind speed increases. Furthermore, increasing TMD mass from 20 to 40 tons causes even larger standard deviation of deflection in the fully loaded region. This means that increasing the mass of TMD does not necessarily improve the performance of this kind of structural controller as it results in higher flexibility of the system.

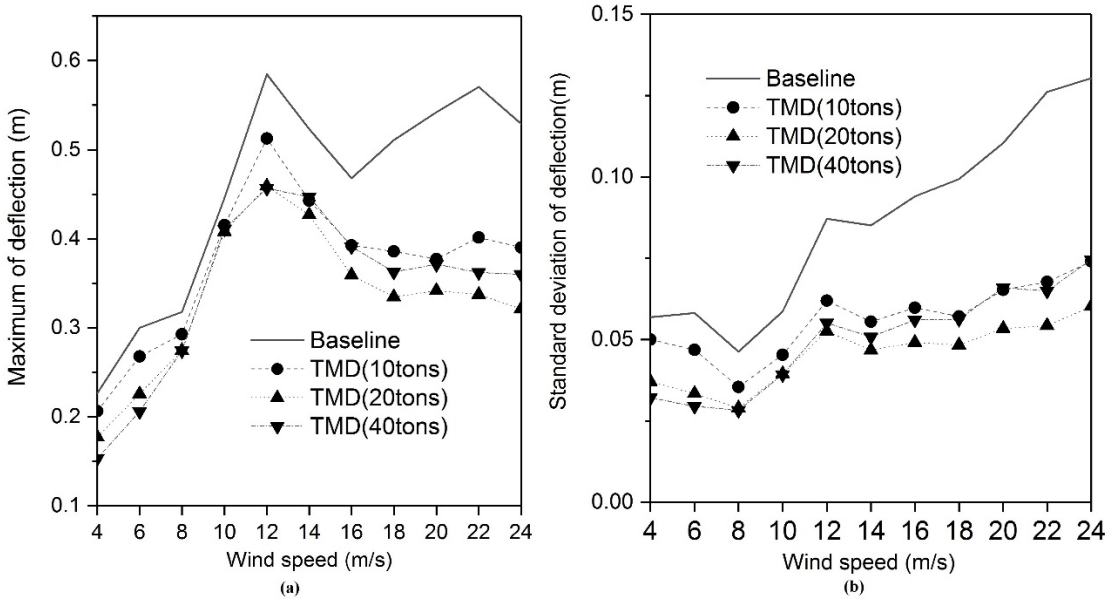

Fig. 13. Deflection in operational conditions using TMDs (a) maximum (b) standard deviation

Next, similar simulations were performed for the systems controlled with TLCDs at different wind speeds and the results are depicted in Fig. 14. As can be seen in this figure, TLCDs are effective in reducing the standard deviation of deflections at all wind speeds. Again increasing the mass of liquid in the optimal TLCD from 20 tons to 40 tons does not improve their suppression effects.

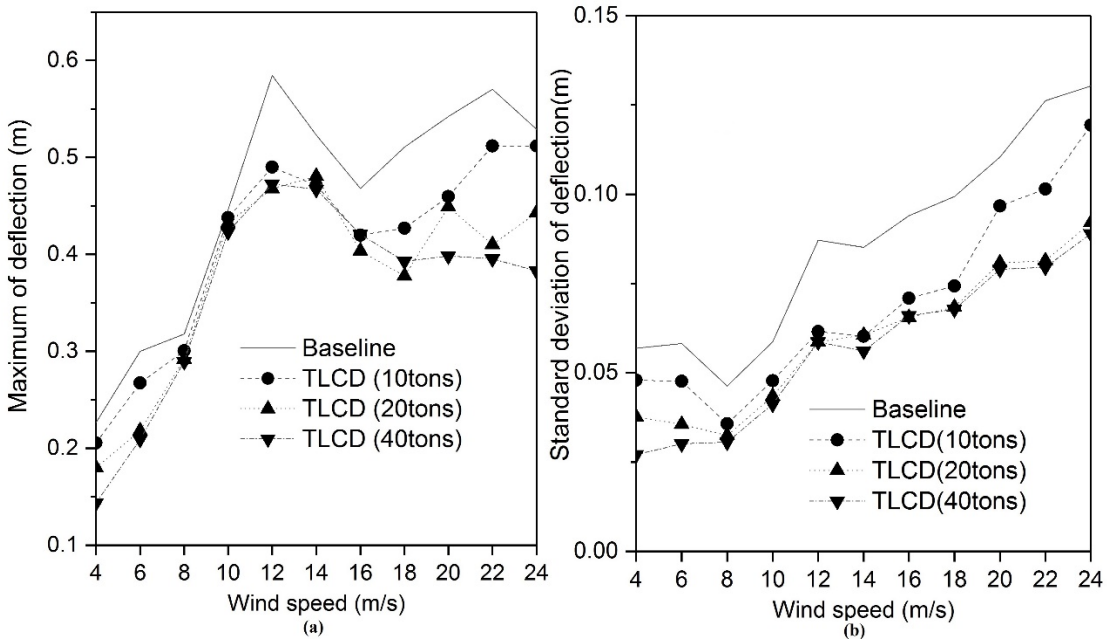

Fig. 14. Deflection in operational conditions using TLCDs (a) maximum (b) standard deviation

Fig. 15. compares the performances of TMD, TLD, and TLCD-TMDs with equal masses (20 tons) at different wind speeds compared to the uncontrolled system. The peak deflections (Fig. 15a) and standard deviation of deflections (Fig. 16b) are suppressed, however standard deviations experienced more significant reductions. At the rated wind speed, a combination of TMD and TLCD outperforms other devices in vibration control with 24 percent decrease in the peak deflections. In the partially loaded region, the curves for three vibration control devices are close to each other. It can be seen that the optimal TMD shows a better performance in operational conditions compared to the TLCDs.

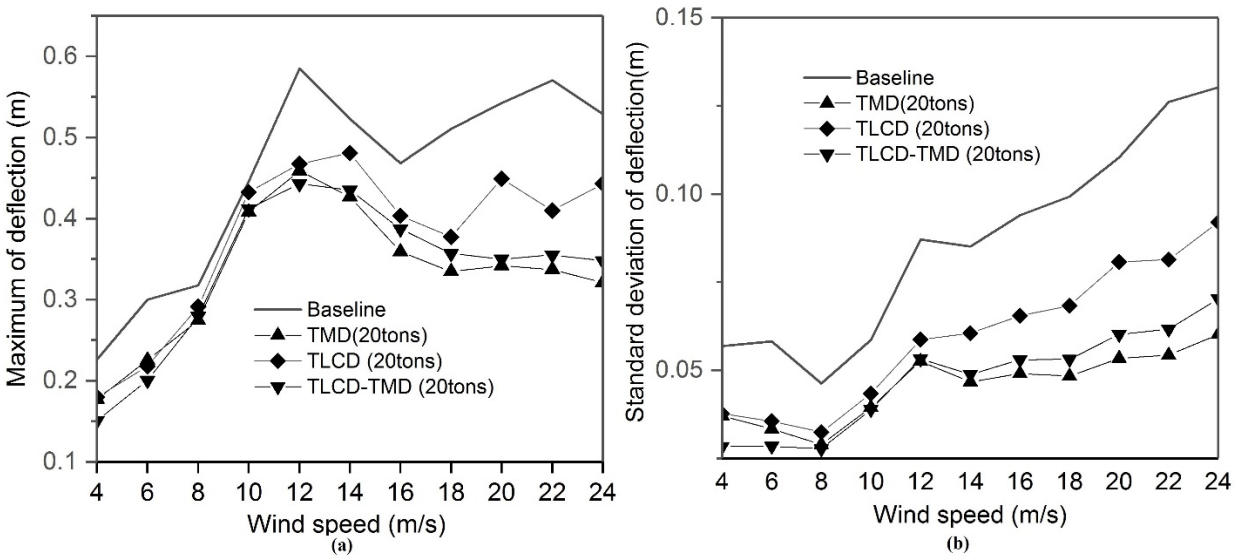

Fig. 15. Deflection in operational conditions using TMD, TLCD, and TLCD-TMD (a) maximum (b) standard deviation

The trend for the standard deviation of deflections in terms of effectiveness of structural control devices is similar to those of maximum of peaks; with the optimal TMD showing better performance in the suppression of vibration followed by TLCD-TMD and TLCD. Also, a weaker performance of TLCDs at high operational wind speed is again proven for the standard deviation of deflection. The summary of the standard deviation of responses (absolute values and reduction percentage compared to the uncontrolled system) for different structural control devices at operational wind speeds are listed in Table 5. The optimal TLCD-TMD system has higher reduction percentage of standard deviation in all cases compared to TLCDs.

Table 5 Standard deviation of deflection for operational wind speed for TMD, TLCD, and TLCD-TMD (20tons)

Wind Speed (m/s)	Baseline	TLCD (20 tons)	TMD (20 tons)	TLCD-TMD (20 tons)
4	0.057	0.038(34%)	0.037(35%)	0.028(50%)
6	0.058	0.036(39%)	0.033(43%)	0.028(51%)
8	0.046	0.032(30%)	0.029(37%)	0.028(40%)
10	0.059	0.043(26%)	0.039(33%)	0.039(34%)
12	0.087	0.059(33%)	0.053(40%)	0.053(39%)
14	0.085	0.061(29%)	0.047(45%)	0.049(43%)
16	0.094	0.066(30%)	0.049(48%)	0.053(44%)
18	0.099	0.068(31%)	0.048(51%)	0.053(46%)
20	0.110	0.081(27%)	0.053(52%)	0.060(45%)
22	0.126	0.081(35%)	0.054(57%)	0.062(51%)
24	0.130	0.092(29%)	0.060(54%)	0.070(46%)

3.4.2. Non-Operational Conditions

In non-operational loading conditions, rotors are not rotating and causing insignificant aerodynamic damping. Since aerodynamic damping is the biggest contributor to total damping in operational conditions, lack of this damping in non-operational conditions causes lower total damping and therefore results in high fatigue damage. Due to high frequency of occurrence of non-operational loading conditions and their high contribution to the total fatigue damage, the non-operational conditions such as parked condition can be considered design drivers. In this section, the effects of structural control devices on the responses of offshore wind turbine systems in parked condition are presented at different wind speeds. For the parked condition, the blades are feathered during the entire simulation. Fig. 16 compares the maximum and standard deviation of deflection at the top of the tower equipped with TMD, TLCD and combined TLCD-TMD with the uncontrolled system under parked conditions at different wind speeds. All vibration control devices reduce the peak and standard deviation values of responses to a great extent except for the TLCD at wind speed of 4m/s. In comparison, the vibration control devices have much higher positive performance under parked conditions due to the absence of aerodynamic damping and additional damping caused by these devices.

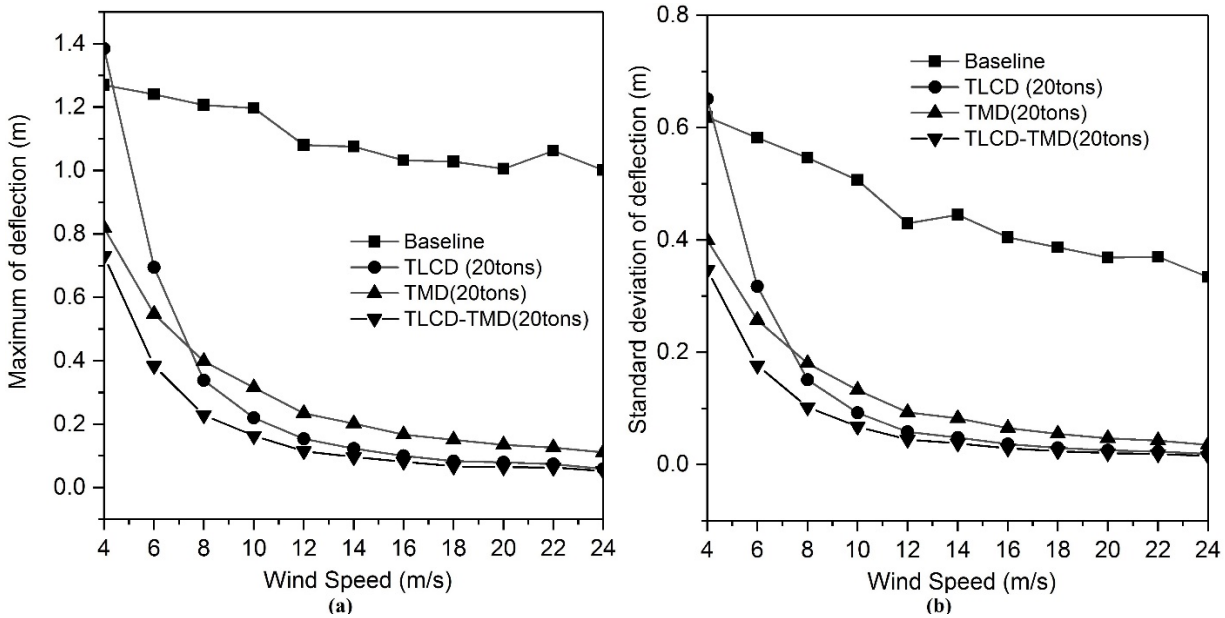

Fig. 16. Deflection in non-operational conditions using TMD, TLCD, and TLCD-TMD (a) maximum (b) standard deviation

The percentage of reduction of the deflection compared to the uncontrolled system is demonstrated in Fig. 17. It can be seen that TLCDs have better performance than TMDs at wind speeds higher than 6 m/s. In addition, the combined TLCD-TMD device has better performance than the rest of the devices, with the maximum of 93% reduction in the standard deviation of the responses for 24 m/s wind speed. Furthermore, there are trends in data to suggest that improvement percentage increases as wind speed increases.

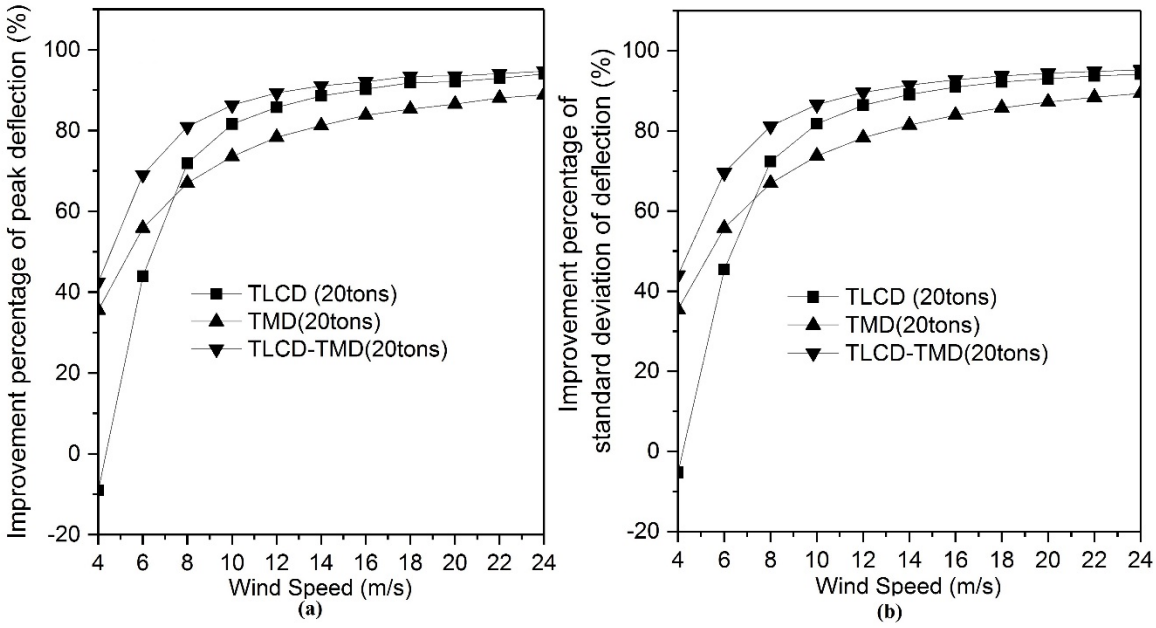

Fig. 17. Improvement percentage of (a) maximum (b) standard deviation of deflection in non-operational conditions with TMD, TLCD, and TLCD-TMD

3.4.3. Startup and Shutdown Conditions

Wind turbines are switched on and off constantly in their lifetime due to weather conditions, maintenance, and other reasons. Therefore, it is important to investigate the effect of structural control devices on the offshore wind turbines in startup and shutdown conditions. The wind turbine studied in this research is controlled using a pitch-to-feather system. For startup conditions, the blades are pitched from feather (90º) to the run positions (12º) with a pitching rate of 2 deg/s during a time span of 39 sec allowing the wind to accelerate the rotor. To simulate shutdown conditions, the blades are pitched from normal angle (12º) to the feathered angle (90º).

Fig. 18 displays a representative 50 s time history of responses of the system after initiating the turbine at rated and cut-off wind speed using the mentioned structural control devices tuned to the first natural frequency of the system. The structural control devices show positive performances in startup condition and this improvement is more pronounced at rated wind speed with the combined TLCD-TMD device.

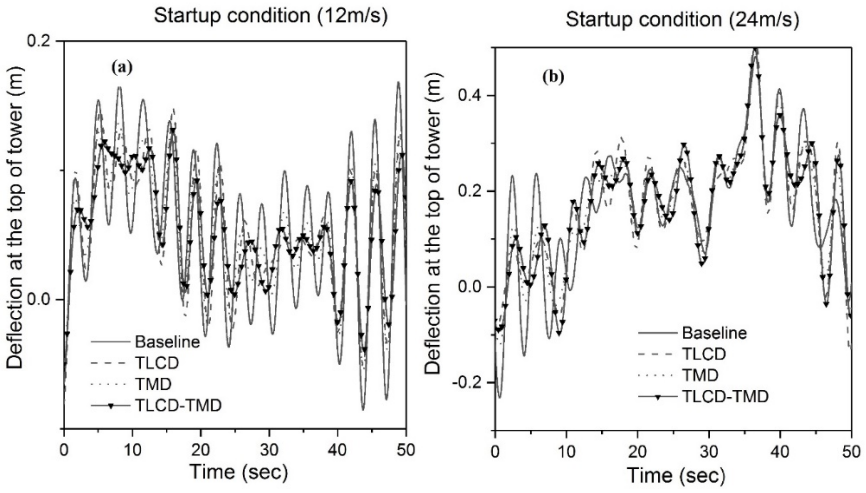

Fig. 18. Time history of deflection in startup condition at wind speed (a) 12m/s (b) 24m/s using TMD, TLCD, and TLCD-TMD

The shutdown condition is assumed as normal with a pitch rate of 2 deg/s in which the blades are pitched from 12º to 90º during a time span of 39 sec. Fig. 19. compares the responses of the controlled and uncontrolled system under shutdown condition. The structural control devices improve the structural responses, with the maximum improvement observed at rated wind speed (Fig. 19a). In comparison, at the cut-off wind speed (Fig. 19b) the optimal TLCD shows negative performance in some part of the time history, whereas the optimal TLCD-TMD is proved to outperform other devices during the whole time span.

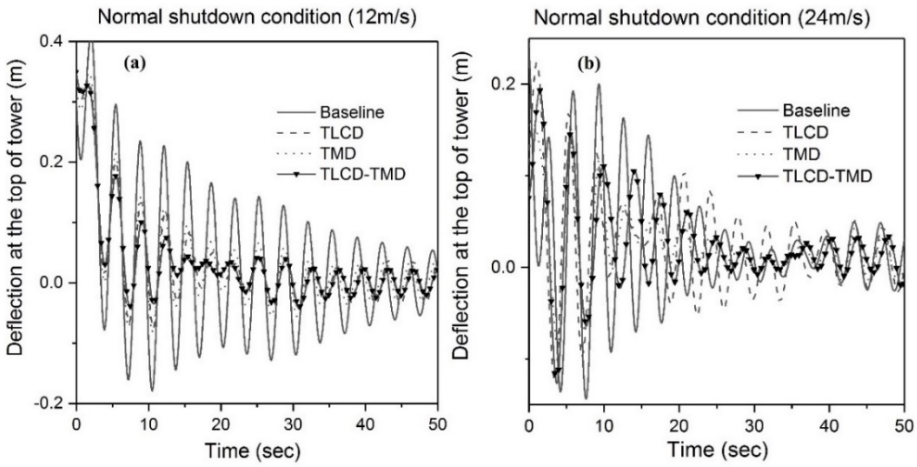

Fig. 19. Time history of deflection in shutdown condition at wind speed (a) 12m/s (b) 24m/s using TMD, TLCD, and TLCD-TMD

4. CONCLUSION

In this study, the use of two passive structural control devices, i.e. tuned mass dampers and tuned liquid column dampers, in fixed offshore wind turbine foundations was investigated. A multiple lumped mass model for jacket foundations including structural control devices was developed. First, OWT foundation was subjected to various loading including initial perturbation, monotonic, impulsive, and harmonic loading conditions. A parametric study of the mentioned structural control devices was performed. Next, stochastic wind loading was applied to the system at various wind speeds for operational, parked, startup and shutdown conditions. The main findings of this study are as follows:

1. The optimal TMD has higher damping contribution to the total damping of the system compared to the system with the optimal TLCD in free decay vibration.
2. The results show that heavier tuned mass dampers dampen out a wider range of applied frequencies, however, they increase the vibration amplitudes for loading frequencies outside that bandwidth in a larger extent.
3. In operational conditions, the optimal TMD outperforms other devices as the standard deviations of the responses are reduced more than 55% when the liquid mass was 20 tons. The optimal TLCD-TMD and TLCD are in the next orders with the maximum of 51% and 39% reduction, respectively.
4. In parked conditions, all the devices show greater performances compared to the operational conditions due to the absence of aerodynamic damping and presence of loading with frequencies closer to the frequency in which the devices are tuned to. This performance gets better when wind speed increases with the maximum of 93% reduction in the standard deviation of

deflection at wind speed 24 m/s for the TLCDs. Furthermore, TLCDs show higher vibration suppression capacity than TMDs in all wind speeds.

5. In startup and shutdown conditions, all control devices show positive performance in attenuating dynamic responses at rated wind speed. However, the optimal TLCD causes a slight increase in the responses at the cut-off wind speed due to its inability to adjust to the highly dynamic motion of the structure.
6. Since TMDs are more efficient in operational conditions, and TLCDs have better performance in parked conditions and due to the fact that the total fatigue damage is caused by the contribution of all the conditions, the combined TLCD-TMD can introduce better overall performance in whole lifetime of the system. The combined system can consist of a TMD installed in the nacelle and a TLCD installed inside the tower. To apply the combined TLCD-TMD in practice, more comprehensive studies with a focus on experimental investigations may be useful.

ACKNOWLEDGEMENT

The authors would like to acknowledge the University of Strathclyde scholarship to carry out this research.

REFERENCES

Bauer, H. F. (1984). Oscillations of immiscible liquids in a rectangular container: a new damper for excited structures. *Journal of Sound and Vibration, 93*(1), 117-133.

Brodersen, M.L., A.S. Bjørke, and J. Høgsberg (2017), *Active tuned mass damper for damping of offshore wind turbine vibrations.* Wind Energy, . **20**(5): p. 783-796.

Colwell, S., & Basu, B. (2009). Tuned liquid column dampers in offshore wind turbines for structural control. *Engineering Structures, 31*(2), 358-368. doi:http://dx.doi.org/10.1016/j.engstruct.2008.09.001

Commission, I. E. (2009). IEC 61400 Design requirements for offshore wind turbines.

Dinh, V.-N., & Basu, B. (2015). Passive control of floating offshore wind turbine nacelle and spar vibrations by multiple tuned mass dampers. *Structural Control and Health Monitoring, 22*(1), 152-176. doi:10.1002/stc.1666

Eddanguir, A., & Benamar, R. (2013). A Discrete Model for Transverse Vibration of a Cantilever Beam Carrying Multi Lumped Masses: Analogy with the Continuous Model. In M. Haddar, L. Romdhane, J. Louati, & A. Ben Amara (Eds.), *Design and Modeling of*

Mechanical Systems: Proceedings of the Fifth International Conference Design and Modeling of Mechanical Systems, CMSM'2013, Djerba, Tunisia, March 25-27, 2013 (pp. 89-96). Berlin, Heidelberg: Springer Berlin Heidelberg.

Er Ming He, Y. Q. H., Yang Zhang, Ge Liang Yin. (2014). Vibration and Load Suppression of Offshore Floating Wind Turbine. *Advanced Materials Research, 1025-1026*, 891-896. doi:10.4028/www.scientific.net/AMR.1025-1026.891

Fitzgerald, B., & Basu, B. (2013). Active Tuned Mass Damper Control of Wind Turbine Nacelle/Tower Vibrations with Damaged Foundations. *Key Engineering Materials, 569-570*, 660-667. doi: 10.4028/www.scientific.net/KEM.569-570.660

Fitzgerald, B., Basu, B., & Nielsen, S. R. K. (2013). Active tuned mass dampers for control of in-plane vibrations of wind turbine blades. *Structural Control and Health Monitoring, 20*(12), 1377-1396. doi:10.1002/stc.1524

Fitzgerald, B., S. Sarkar, and A. Staino, (2018) *Improved reliability of wind turbine towers with active tuned mass dampers (ATMDs)*. Journal of Sound and Vibration. **419**: p. 103-122.

Fujino, Y., Sun, L., Pacheco, B. M., & Chaiseri, P. (1992). Tuned liquid damper (TLD) for suppressing horizontal motion of structures. *Journal of Engineering Mechanics, 118*(10), 2017-2030.

Ghaemmaghami, A. R., Kianoush, R., & Mercan, O. (2015). Numerical modeling of dynamic behavior of annular tuned liquid dampers for the application in wind towers under seismic loading. *Journal of Vibration and Control, 22*(18), 3858-3876. doi:10.1177/1077546314567524

J, A., & B, B. (2007). *Vibration control of wind turbine blades using tuned liquid dampers*. Paper presented at the the eleventh international conference on civil, structural and environmental, engineering computing, Stirlingshire, UK.

J. Jonkman, S. B., W. Musial, and G. Scott. (2009). *Definition of a 5-MW Reference Wind Turbine for Offshore System Development*. Retrieved from

John, A., Vikram, P., Biswajit, B., & Satish, N. (2011). Control of flapwise vibrations in wind turbine blades using semi-active tuned mass dampers. *Structural Control and Health Monitoring, 18*(8), 840-851. doi:doi:10.1002/stc.404

Jonkman, B. J. (2009). *TurbSim user's guide: Version 1.50*. Retrieved from

Jonkman, J. M., & Buhl Jr, M. L. (2005). *FAST User's Guide-Updated August 2005*. Retrieved from

Kaimal, J. C., Wyngaard, J. C., Izumi, Y., & Coté, O. R. (1972). Spectral characteristics of surface-layer turbulence. *Quarterly Journal of the Royal Meteorological Society, 98*(417), 563-589. doi:doi:10.1002/qj.49709841707

Kareem, A., Kijewski, T., & Tamura, Y. (1999). Mitigation of motions of tall buildings with specific examples of recent applications. *Wind and structures, 2*(3), 201-251.

Lackner, M. A., & Rotea, M. A. (2011a). Passive structural control of offshore wind turbines. *Wind Energy, 14*(3), 373-388. doi:10.1002/we.426

Lackner, M. A., & Rotea, M. A. (2011b). Structural control of floating wind turbines. *Mechatronics, 21*(4), 704-719. doi:https://doi.org/10.1016/j.mechatronics.2010.11.007

Lepelletier, T., & Raichlen, F. (1988). Nonlinear oscillations in rectangular tanks. *Journal of Engineering Mechanics, 114*(1), 1-23.

Mensah, A. F., & Dueñas-Osorio, L. (2014). Improved reliability of wind turbine towers with tuned liquid column dampers (TLCDs). *Structural Safety, 47*, 78-86. doi:http://dx.doi.org/10.1016/j.strusafe.2013.08.004

Newmark, N. M. (1959). A method of computation for structural dynamics. *Journal of the engineering mechanics division, 85*(3), 67-94.

Sakai, F., Takeda, S., & Tamaki, T. (1989). *Tuned liquid column damper-new type device for suppression of building vibrations.* Paper presented at the Highrise Buildings, Nanjing, China.

Seidel, M. (2014). Substructures for Offshore Wind Turbines–Current Trends and Developments. *Festschrift Peter Schaumann*, 363-368.

Stewart, G., & Lackner, M. (2013). Offshore Wind Turbine Load Reduction Employing Optimal Passive Tuned Mass Damping Systems. *IEEE Transactions on Control Systems Technology, 21*(4), 1090-1104. doi:10.1109/TCST.2013.2260825

Stewart, G. M., & Lackner, M. A. (2014). The impact of passive tuned mass dampers and wind–wave misalignment on offshore wind turbine loads. *Engineering Structures, 73*, 54-61. doi:http://dx.doi.org/10.1016/j.engstruct.2014.04.045

Sun, C. (2018). Semi-active control of monopile offshore wind turbines under multi-hazards. *Mechanical Systems and Signal Processing, 99*, 285-305. doi:https://doi.org/10.1016/j.ymssp.2017.06.016

Symans, M. D., & Constantinou, M. C. (1999). Semi-active control systems for seismic protection of structures: a state-of-the-art review. *Engineering Structures, 21*(6), 469-487. doi:https://doi.org/10.1016/S0141-0296(97)00225-3

Vorpahl, F. (2013). *Description of a basic model of the `UpWind reference jacket' for code comparison in the OC4 project under IEA Wind Annex 30*. Retrieved from

Welt, F., & Modi, V. (1992). Vibration damping through liquid sloshing, Part I: a nonlinear analysis. *Journal of vibration and acoustics, 114*(1), 10-16.

Wu, J.-C., Shih, M.-H., Lin, Y.-Y., & Shen, Y.-C. (2005). Design guidelines for tuned liquid column damper for structures responding to wind. *Engineering Structures, 27*(13), 1893-1905. doi:https://doi.org/10.1016/j.engstruct.2005.05.009

Yalla, S. K., & Kareem, A. (2000). Optimum absorber parameters for tuned liquid column dampers. *Journal of Structural Engineering, 126*(8), 906-915.

Hu, Y. and E. He, (2017). *Active structural control of a floating wind turbine with a stroke-limited hybrid mass damper.* Journal of Sound and Vibration, 2017. **410**: p. 447-472.

Yilmaz, O. C. (2012). *The Optimization of Offshore Wind Turbine Towers Using Passive Tuned Mass Dampers.* (MASTER OF SCIENCE), University of Massachusetts.

Zhang, Z., Basu, B., & Nielsen, S. R. K. (2015). Tuned liquid column dampers for mitigation of edgewise vibrations in rotating wind turbine blades. *Structural Control and Health Monitoring, 22*(3), 500-517. doi:10.1002/stc.1689

Zuo, H., Bi, K., & Hao, H. (2017). Using multiple tuned mass dampers to control offshore wind turbine vibrations under multiple hazards. *Engineering Structures, 141*, 303-315. doi:https://doi.org/10.1016/j.engstruct.2017.03.006

APPENDIX:

The stiffness and mass matrices of the main structure used in this study are given as follows respectively:

$$
[K_s]=\begin{bmatrix}
E\left(\frac{3I_1}{h_1^3}+\frac{4I_2}{h_2^3}+\frac{I_3}{h_3^3}\right) & -2E\left(\frac{I_1}{h_1^3}+\frac{I_2}{h_2^3}\right) & E\frac{I_2}{h_2^3} & 0 & 0 & 0 & & & 0 \\
-2E\left(\frac{I_1}{h_1^3}+\frac{I_2}{h_2^3}\right) & E\left(\frac{I_2}{h_2^3}+\frac{4I_3}{h_3^3}+\frac{I_4}{h_4^3}\right) & -2E\left(\frac{I_2}{h_2^3}+\frac{I_3}{h_3^3}\right) & E\frac{I_3}{h_3^3} & 0 & 0 & & & \\
E\frac{I_2}{h_2^3} & -2E\left(\frac{I_2}{h_2^3}+\frac{I_3}{h_3^3}\right) & E\left(\frac{I_3}{h_3^3}+\frac{4I_4}{h_4^3}+\frac{I_5}{h_5^3}\right) & & & & & & \\
0 & E\frac{I_3}{h_3^3} & & & & & & & \\
 & 0 & & & & & & E\frac{I_{N-2}}{h_{N-2}^3} & \\
 & & & & -2E\left(\frac{I_{N-3}}{h_{N-3}^3}+\frac{I_{N-2}}{h_{N-2}^3}\right) & E\left(\frac{I_{N-2}}{h_{N-2}^3}+\frac{4I_{N-1}}{h_{N-1}^3}+\frac{I_N}{h_N^3}\right) & -2E\left(\frac{I_{N-2}}{h_{N-2}^3}+\frac{I_{N-1}}{h_{N-1}^3}\right) & E\frac{I_{N-1}}{h_{N-1}^3} \\
 & & & & E\frac{I_{N-2}}{h_{N-2}^3} & -2E\left(\frac{I_{N-2}}{h_{N-2}^3}+\frac{I_{N-1}}{h_{N-1}^3}\right) & E\left(\frac{I_{N-1}}{h_{N-1}^3}+\frac{4I_N}{h_N^3}\right) & -2E\frac{I_N}{h_N^3} \\
 & 0 & & & 0 & E\frac{I_{N-1}}{h_{N-1}^3} & -2E\frac{I_N}{h_N^3} & E\frac{I_N}{h_N^3}
\end{bmatrix} \tag{A.1}
$$

$$
[M_s]=\begin{bmatrix}
m_1 & 0 & 0 & & & 0 & 0 \\
0 & m_2 & 0 & & & & \\
0 & 0 & m_3 & & & & \\
 & & & & & & \\
 & & & & & 0 & 0 \\
 & & & & 0 & m_{N-1} & 0 \\
0 & 0 & & & 0 & 0 & m_N
\end{bmatrix} \tag{A.2}
$$